Conductive Polymeric Porphyrin Films: Application in the Electrocatalytic Oxidation of Hydrazine

J. E. Bennett and T. Malinski*

Department of Chemistry, Oakland University, Rochester, Michigan 48309-4401

Received December 3, 1990. Revised Manuscript Received February 6, 1991

Conductive polymeric porphyrin films have been obtained by oxidative electropolymerization of two major groups of porphyrin complexes. The first group is composed of several novel porphyrin systems: *meso*-[2.2]paracyclophanyltriphenylporphyrin, PCPP, with Co as the central metal, and *meso*-tetrakis-[2.2]paracyclophanylporphyrin, T(PCP)P, with Fe, Co, Mn, and Ni as central metals. The second group comprises the free-base and metalated tetrakis(*p*-(diethylamino)phenyl)porphyrins with Cu, Fe, Co, Mn, Ni, and Pd as central metals and the Ru carbonyl pyridinate analogue of this porphyrin group with carbonyl and *tert*-butylpyridine (*t*-Bupy) as axial ligands, general formula M(*p*-Et_2N)TPP. This work focuses on two important aspects of the porphyrin films, their surface morphology as viewed by scanning electron microscopy and their catalytic activity in regard to the electrocatalytic oxidation of hydrazine. The films presented in the morphology discussion are those electropolymerized from T(PCP)P, Ru(CO)(*p*-Et_2N)-TPP(*t*-Bupy), and Co(*p*-Et_2N)TPP. The films used in the catalytic studies on hydrazine oxidation are those electropolymerized from PCPP, CoPCPP, both T(PCP)P and M(*p*-Et_2N)TPP with Co, Mn, and Ni as central metals, and Ru(CO)(*p*-Et_2N)TPP(*t*-Bupy).

Introduction

The role of metalloporphyrins as a model for the iron porphyrin unit present in heme proteins and for use as possible electrocatalysts is well established.[1-9] Although metalloporphyrins are applicable in both homogeneous and heterogeneous catalysis,[10-14] the fact that oxygen can be reduced directly via a four-electron pathway on some transition-metal porphyrins has focused attention on the heterogeneous electrocatalytic oxygen reduction reaction.[1,5,8,9,15] For metalloporphyrins to be useful in heterogeneous electrocatalysis, successful attachment to solid electrodes must be attained, and this can be realized by various methods, with the method of electrochemical polymerization offering not only simplicity for the synthesis of polymeric porphyrins but direct formation of possible electroactive, adherent, and stable films on solid electrodes.

Since the discovery that aniline, pyrrole, and phenol can form electroactive polymer films, there has been considerable interest in the amino-, pyrrole-, and hydroxy-substituted porphyrins, especially in regard to those that can form films via oxidative or reductive electropolymerization, and several poly films formed from the amino-, pyrrole-, and hydroxy-substituted porphyrins have been reported.[1,7,8,16] Pertinent to these studies, poly-Co-tetrakis(*o*-aminophenyl)porphyrin films[1] are particularly effective catalysts for the electroreduction of oxygen in aqueous media, and poly-Ni-tetrakis(3-methoxy-4-hydroxyphenyl)porphyrin films are applicable as an anode for the catalytic oxidation of water and methanol in basic media.[16]

Research in the electrocatalysis of film electrodes has generally focused on the electroreduction of dioxygen and the catalytic oxidation of water and methanol, owing to the significance of these reactions in regard to energy conversion and storage. Much less attention has been given to another important reaction in the area of energy conversion and storage, and that is the electrocatalytic oxidation of hydrazine. Previous reports on this reaction have concentrated more on the mechanisms of the reaction rather than with electrocatalytic effects of the polymeric materials involved.[17-19]

The focus of this report is on porphyrin films formed by oxidative polymerization of two major groups of porphyrin systems. The first group comprises several novel porphyrin systems: the free-base and metalated *meso*-[2.2]paracyclophanyltriphenylporphyrin, PCPP,[20,21] with

* To whom correspondence should be addressed.

(1) Bettelheim, A.; White, B. A.; Raybuck, S. A.; Murray, R. W. *Inorg. Chem.* **1987**, *26*, 1009 and references therein.
(2) Buttry, D. A.; Anson, F. C. *J. Am. Chem. Soc.* **1984**, *106*, 59.
(3) Kuwana, T.; Fujihira, M.; Sunakawa, K.; Osa, T. *J. Electroanal. Chem.* **1978**, *83*, 207.
(4) Bettelheim, A.; Chan, R. J. H.; Kuwana, T. *J. Electroanal. Chem.* **1979**, *99*, 391.
(5) Bettelheim, A.; Chan, R. J. H.; Kuwana, T. *J. Electroanal. Chem.* **1980**, *110*, 93.
(6) Macor, K. A.; Spiro, T. G. *J. Am. Chem. Soc.* **1983**, *105*, 5601.
(7) White, B. A.; Murray, R. W. *J. Electroanal. Chem.* **1985**, *189*, 345.
(8) Bettelheim, A.; White, B. A.; Murray, R. W. *J. Electroanal. Chem.* **1987**, *217*, 271.
(9) Macor, K. A.; Su, Y. O.; Miller, L. A.; Spiro, T. G. *Inorg. Chem.* **1987**, *26*, 2594.
(10) Brodd, R. J.; Leger, V. Z.; Scarr, R. F.; Kozawa, A. National Bureau of Standards Special Publications, 455, Proceedings of Workshop held at NBS, Gaithersburg, MD, 1976; p 253.
(11) (a) Andrieux, C. P.; Dumas-Bouchiat, J. M.; Saveant, J. M. *J. Electroanal. Chem.* **1980**, *114*, 159; (b) Ibid. **1980**, *123*, 171; (c) Ibid. **1982**, *131*, 1.
(12) Saveant, J. M.; Anson, F. C.; Shigehara, K. *J. Phys. Chem.* **1983**, *87*, 214.
(13) Andrieux, C. P.; Saveant, J. M. *J. Electroanal. Chem.* **1982**, *134*, 163.
(14) Groves, J. T. In *Catalysis of Organic Reactions*; Moser, W. R., Ed.; Marcel Dekker: New York, 1981; p 131.
(15) Spiro, T. G., Ed. *Metal Ion Activation of Dioxygen*; Wiley-Interscience: New York, 1980.
(16) (a) Malinski, T.; Ciszewski, A.; Bennett, J. E.; Czuchajowski, L. 176th Meeting of The Electrochemical Society, Hollywood, FL, 1989; extended abstract 24. (b) Malinski, T.; Ciszewski, A.; Bennett, J. E.; Czuchajowski, L. In *Proceedings of the Symposium on Nickel Hydroxide Electrodes*; Corrigan, D. A., Zimmerman, A. H., Eds.; The Electrochemical Society Inc.: Pennington, NJ, 1989.
(17) (a) Zagal, J.; Lira, S.; Ureta-Zanartu, S. *J. Electroanal. Chem.* **1986**, *210*, 95. (b) Zagal, J.; Munoz, E.; Ureta-Zanartu, S. *Electrochim. Acta* **1982**, *27*, 1373. (c) Zagal, J.; Fierro, C.; Munoz, E.; Rozas, R.; Ureta-Zanartu, S. In *Proceedings of the Symposium on Electrocatalysis*; O'Grady, W. E., Ross, Jr., P. N., Will, F. G., Eds.; The Electrochemical Society Inc.: Pennington, NJ, 1982, p 389. (d) Zagal, J. *J. Electroanal. Chem.* **1980**, *109*, 389. (e) Zagal, J.; Ureta-Zanartu, S. *J. Electrochem. Soc.* **1982**, *127*, 2242. (f) Zagal, J.; Herrera, P.; Brinck, K.; Munoz, E.; Ureta-Zanartu, S. In *Proceedings of the Symposium on Chemistry and Physics of Electrocatalysis*; McIntyre, J. D. E., Weaver, M. J., Yeager, E., Eds.; The Electrochemical Society Inc.: Pennington, NJ, 1982; p 602.
(18) Jannakoudakis, A. D.; Kokkinidis, G. *J. Electroanal. Chem.* **1982**, *134*, 311.
(19) Kodera, T.; Honda, M.; Kita, H. *Electrochimica Acta* **1985**, *30*, 669.
(20) Czuchajowski, L.; Goszczynski, S.; Wheeler, D. E.; Wisor, A. K.; Malinski, T. *J. Heterocycl. Chem.* **1988**, *25*, 1825.
(21) Wheeler, D. E. Ph.D. Thesis, University of Idaho, Moscow, ID, 1990; private communication.

0897-4756/91/2803-0490$02.50/0

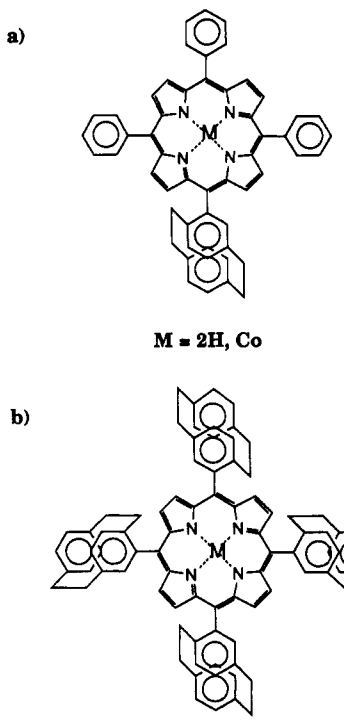

Figure 1. (a) Structure of *meso*-[2.2]paracyclophanyltriphenylporphyrin, PCPP; (b) structure of *meso*-tetrakis[2.2]-paracyclophanylporphyrin, T(PCP)P.

Co as the central metal, and *meso*-tetrakis[2.2]paracyclophanylporphyrin, T(PCP)P,[21,22] with Co, Mn and Ni as central metals, which consist of [2.2]paracyclophane units directly attached to the porphyrin core. The second group consists of the free-base and metalated tetrakis(*p*-(diethylamino)phenyl)porphyrins with Co, Mn, and Ni as central metals and the Ru carbonyl pyridinate analogue of this porphyrin group with carbonyl (CO) and *tert*-butylpyridine (*t*-Bupy) as axial ligands, general formula M(*p*-Et_2N)TPP. This report presents not only our results obtained in the electrocatalytic oxidation of hydrazine with films on glassy carbon electrodes but also the morphology of several of these same films on platinum electrodes. The films presented in the morphology discussion are those electropolymerized from T(PCP)P, Ru(CO)(*p*-Et_2N)-TPP(*t*-Bupy), and Co(*p*-Et_2N)TPP. The films used in the study of hydrazine oxidation are those formed from PCPP, CoPCPP, both T(PCP)P and M(*p*-Et_2N)TPP with Co, Mn, and Ni as central metals, and Ru(CO)(*p*-Et_2N)TPP-(*t*-Bupy), Figures 1 and 2.

Experimental Section

Preparation of Porphyrins and Metalloporphyrins. *meso*-[2.2]Paracyclophanyltriphenylporphyrin, PCPP, was synthesized following the method of Adler et al.,[23] by a mixed condensation of pyrrole (40 mmol) and propionic acid (350 mL, reflux 1 h) with benzaldehyde (30 mmol) and [2.2]paracylophane-4-carbaldehyde (10 mmol).[24] The separational procedures, as well as the spectral properties and the metalations have been described in detail elsewhere.[20,21,25]

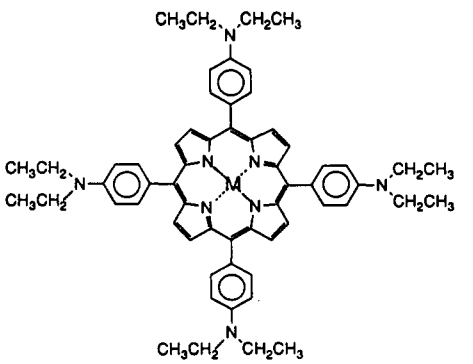

Figure 2. Structure of the metalated *meso*-tetrakis(*p*-(diethylamino)phenyl)porphyrin, M(*p*-Et_2N)TPP.

meso-Tetrakis[2.2]paracyclophanylporphyrin, T(PCP)P, was synthesized as a mixture of stereoisomers, from (*R*+*S*)[2.2]-paracyclophane-4-carbaldehyde[24] and pyrrole, in chloroform solution at room temperature following the method of Lindsey et al.[26] The complete synthesis, along with the separational procedures, spectral properties, and metalations, have been described previously.[21,22b,27]

The syntheses of tetrakis(*p*-(diethylamino)phenyl)porphyrin, H_2(*p*-Et_2N)TPP, with Pd, Mn, Co, Ni, Cu, and Fe as central metals, as well as the ruthenium carbonyl 4-*tert*-butylpyridinate derivative of tetrakis(*p*-(diethylamino)phenyl)porphyrin, Ru-(CO)(*p*-Et_2N)TPP(*t*-Bupy), were according to the procedure of Eaton and Eaton.[28] In this method, pyrrole was added dropwise to a refluxing mixture of *p*-(diethylamino)phenyl aldehyde ($Et_2NC_6H_4CHO$) in propionic acid.

Materials, Electrodes, and Instrumentation. Tetrabutylammonium perchlorate (TBAP, Eastman Kodak Co) was recrystallized from methanol and water and dried in vacuo for 48 h at 45 °C prior to use. Dichloroethane, $(CH_2)_2Cl_2$, was purchased in anhydrous form (Sureseal, Aldrich) and stored in the dark over activated 4-Å molecular sieves. Hydrazine sulfate ($NH_2NH_2{\cdot}H_2SO_4$), purchased from Aldrich, was used as received.

A three-electrode conventional configuration consisting of a working electrode, a platinum (Pt) auxilliary electrode, and a saturated calomel reference electrode (SCE) was used in all electrochemical experiments. Potentials are reported versus the SCE (−0.241 V versus NHE at 25 °C). The working electrodes used in these studies consisted of a Teflon-shrouded glassy carbon (GC) electrode (area 0.08 cm^2, Bioanalytical Systems) and 5-mm platinum (Pt) disks (area 0.2 cm^2), fashioned in house from Pt foil, 0.25 mm thick (Puritronic, Johnson Matthey). Prior to use, the surface of the Pt and/or GC working electrode was polished sequentially with 1.0-, 0.3-, and 0.05-μm alumina and then placed in an ultrasonic cleaner for 5 min with the solvent chosen for the measurement.

The substrate–solvent system used in the catalytic oxidation of hydrazine was 0.01 M hydrazine sulfate ($NH_2NH_2{\cdot}H_2SO_4$) in 0.1 M NaOH, while the potential scanned for this experiment was −0.2 to +1.1 V.

Morphology studies were performed on films that had been electrochemically desposited on 0.2-cm^2 Pt disks. The films were coated with ca. 10 nm of gold and examined with a Philips PSEM 500 scanning electron microscope.

Electropolymerizations. The polymeric films on both the Pt and the GC electrodes were formed by oxidative electropolymerization from $ClCH_2CH_2Cl$ and 0.1 M TBAP solutions containing 0.5–1.0 mM porphyrin by scanning (100 mV s^{-1}) the working electrode potential between limits as negative as −0.8 V

(22) (a) Czuchajowski, L.; Lozynski, M. J. *J. Heterocycl. Chem.* **1988**, *25*, 349. (b) Czuchajowski, L.; Goszczynski, S.; Wisor, A. K. *J. Heterocycl. Chem.* **1988**, *25*, 1343.

(23) Adler, A. D.; Longo, F. R.; Finarelli, J. D.; Goldmacher, J.; Assour, J.; Korsakoff, L. *J. Org. Chem.* **1967**, *32*, 476.

(24) Hopf, H.; Raulfus, F. W. *Isr. J. Chem.* **1985**, *25*, 210.

(25) Czuchajowski, L.; Bennett, J. E.; Goszczynki, S.; Wheeler, D. E.; Wisor, A. K.; Malinski, T. *J. Am. Chem. Soc.* **1989**, *111*, 607.

(26) Wagner, R. W.; Lawrence, D. S.; Lindsey, J. S. *Tetrahedron Lett.* **1987**, 3069.

(27) Czuchajowski, L.; Goszczynski, S.; Wisor, A. K.; Bennett, J. E.; Malinski, T. *J. Heterocycl. Chem.* **1989**, *26*, 1477.

(28) Eaton, S. S.; Eaton, G. R. *Inorg. Chem.* **1977**, *16*, 72.

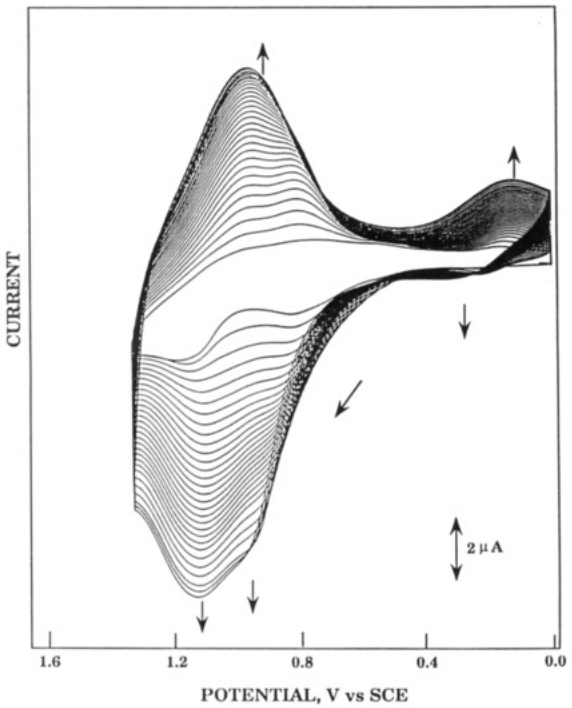

Figure 3. Continuous-scan cyclic voltammogram of Ru(CO)(p-Et_2N)TPP(t-Bupy) from 0.0 to 1.5 V in $(CH_2)_2Cl_2$ (0.1 M TBAP).

to an oxidative potential 1.7 V or by applying a constant potential between 1.3 and 1.7 V for varying time periods. A PAR Model 173 potentiostat and PAR Model 179 coulometer were used for the electrodeposition process and control of film thickness. The quantity of electrodeposited film coverage, Γ (mol cm^{-2}), for M(p-Et_2N)TPP was determined by integration of the charge under the cyclic voltammetric waves or by coulometry; for the PCPP, T(PCP)P, and metalated derivatives, film coverage was determined by coulometry.

Results and Discussion

Overview. Recently, we reported on the oxidative electropolymerization of PCPP, T(PCP)P, and M(p-Et_2N)TPP. Current studies have shown both interesting and unexpected properties in the spectroscopic and electrochemical data of these porphyrin systems.[25,27,29-32] In addition, the electrochemistry, film formation, and film morphology of several of the porphyrins in these two groups have been described, along with an initial report on the conductivity of the porphyrin films via impedance and reflectance spectroscopy.[30-32]

There are several aspects of the poly[(diethylamino)phenyl]porphyrin films that make them different from the polyparacyclophanylporphyrin films. First, the poly-M(p-Et_2N)TPP films electropolymerize easier and faster than any of the free-base or metalated poly-PCPP and poly-T(PCP)P films. This is evident when the continuous scan cyclic voltammograms of M(p-Et_2N)TPP are compared to those of both PCPP and T(PCP)P. Second, while the poly-M(p-Et_2N)TPP films demonstrate distinct voltammetric peaks in $(CH_2)_2Cl_2$/TBAP solution, the free-base poly-PCPP and poly-T(PCP)P films show only broadened and vague cyclic voltammetric waves as was demonstrated previously in refs 25 and 27. Significantly, the metalated poly-PCPP and poly-T(PCP)P films do show broadened voltammetric peaks for the central metal redox couples, similar to those existing in the electrochemistry of the porphyrin solutions.

Table I. Cyclic Voltammetric Peak Potentials and Electrode Coverage for the Oxidation of Metalated Poly-(p-Et_2N)TPP Films on Pt in $(CH_2)_2Cl_2$ (0.1 M TBAP)[a]

compound	potential range for electropolym	peak potential, V vs SCE E_{pa}	E_{pc}	$10^8\Gamma$, mol/cm^2
Co(p-Et_2N)TPP	0.0 → 1.50 V	1.21	0.93	2
Ni(p-Et_2N)TPP	0.0 → 1.80 V	1.18	1.00	1
Ru(CO)(p-Et_2N)TPP-(t-Bupy)	0.0 → 1.30 V	1.20	0.85	5
Mn(p-Et_2N)TPP	0.0 → 1.62 V	1.34	1.17	2

[a] Film coverage was calculated for 30 scans of the potential at a scan rate of 100 mV s^{-1}.

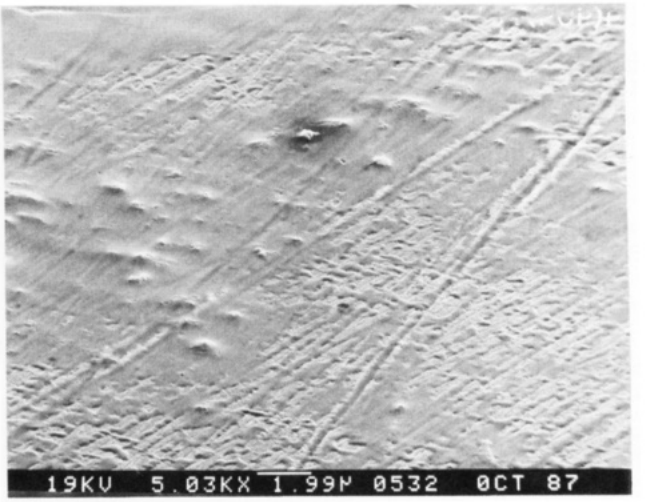

Figure 4. Scanning electron micrograph of a thin T(PCP)P film grown electrochemically on a Pt electrode at a constant potential of 1.6 V; magnification 5000:1.

A typical continuous scan cyclic voltammogram of Ru(CO)(p-Et_2N)TPP(t-Bupy), obtained during film formation, is presented in Figure 3. This figure demonstrates not only that the anodic peak potentials merge and shift in the positive direction but also that the current of the waves grow with each successive scan of the potential. The main wave, which is finally formed as film formation proceeds, is the wave used to determine film thickness by integration of charge. When the film electrodes from the various M(p-Et_2N)TPP are transferred to a $(CH_2)_2Cl_2$/TBAP solution, the cyclic voltammograms show one major redox couple with the anodic peak potentials ranging between 1.20 and 1.34 V and the cathodic peak potentials ranging between 0.85 and 1.17 V. This is true for all of the M(p-Et_2N)TPP film electrodes studied. The peak potentials for the M(p-Et_2N)TPP films, in addition to the film coverage resulting from 30 scans of the potential, are listed in Table I. For a few of the M(p-Et_2N)TPP films, Ru(CO)(p-Et_2N)TPP(t-Bupy) being an example, a minor redox couple is observed between 0.0 and 0.4 V, which is not observed when the film electrode is transferred to an aqueous solution.

Despite the differences existant in the films of the two groups of porphyrins, it is interesting to note that the films formed from PCPP and T(PCP)P, as well as their meta-

(29) Bennett, J. E.; Wheeler, D. E.; Czuchajowski, L.; Malinski, T. *J. Chem. Soc., Chem. Commun.* **1989**, 723.
(30) Malinski, T.; Bennett, J. E. In *Redox Chemistry and Interfacial Behavior of Biological Molecules*; Dryhurst, G., Niki, K., Eds.; Plenum Press: New York, 1988; p 87.
(31) (a) Malinski, T.; Bennett, J. E.; Ciszewski, A.; Czuchajowski, L.; Edwards, W. D.; Wheeler, D. E. 196th ACS National Meeting, Los Angeles, CA; Sept 25–30, 1988, INOR 302. (b) Malinski, T.; Bennett, J. E. Electrochemical Society Meeting, Honolulu, HI, 1987; extended abstract 1285.
(32) Bennett, J. E. Ph.D. Thesis, Oakland University, Rochester, MI, 1990.

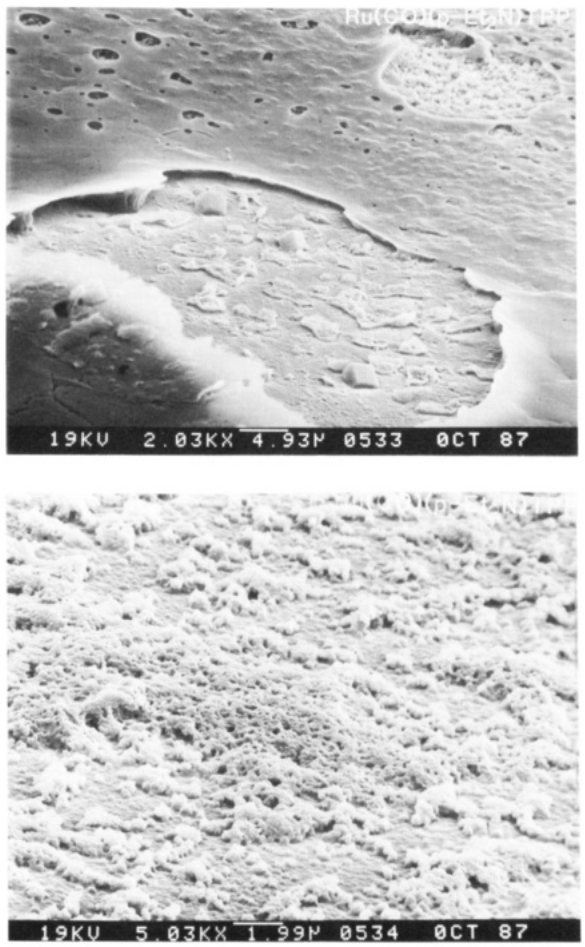

Figure 5. Scanning electron micrographs of a Ru(CO)(p-Et_2N)TPP(t-Bupy) film grown electrochemically on a Pt electrode at a constant potential of 1.45 V for 10 min. Magnifications: (a) 2000:1, (b) 5000:1, from inside the upper right crater that appears in (a).

lated analogues, and the films formed from M(p-Et_2N)-TPP, exhibit catalytic properties toward the electroreduction of dioxygen in aqueous media and the oxidation of hydrazine in basic media. In addition, poly-Co(p-Et_2N)TPP, poly-PCPP, poly-CoPCPP, and the poly-NiT-(PCP)P films show catalytic activity in the oxidation of water in basic media.[32] The fact that both groups of polymeric films not only are highly conductive but also show catalytic activity and are stable in both acidic and basic aqueous solutions as well as in many common nonaqueous solvents, make them possible candidates for application in electrocatalysis and in energy storage devices.

Film Morphology. Figure 4 shows a scanning electron micrograph of a thin T(PCP)P film grown electrochemically on a Pt electrode at a constant potential of 1.6 V, and as can be seen in this micrograph, the morphology of the film appears smooth with no microspheroidical features visible under the electron microscopic magnification of 5000:1. Also noticeable is that the film is somewhat irregular on the electrode surface, with small areas of platinum exposed in the polymer field. This is quite a constrast from the morphology of both the Ru(CO)(p-Et_2N)TPP(t-Bupy) and the Co(p-Et_2N)TPP films grown electrochemically on Pt electrodes, which show no platinum exposed in the polymer field and, in fact, are a great deal thicker, by at least a factor of 10, than the T(PCP)P film. A scanning electron micrograph, Figure 5a, of polymeric Ru(CO)(p-Et_2N)TPP(t-Bupy) reveals a relatively smooth, caramellike-looking surface, containing

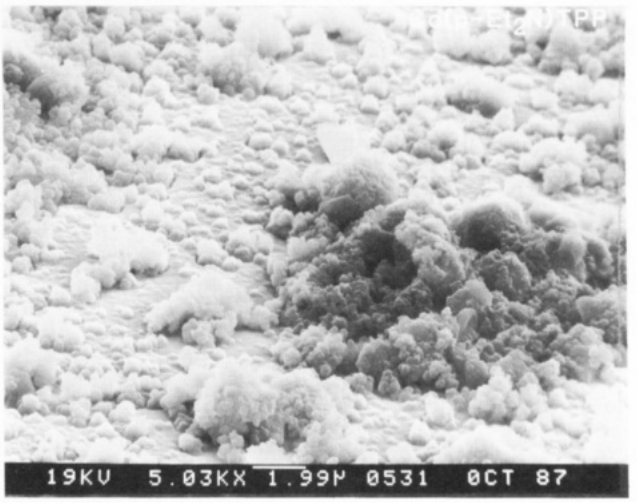

Figure 6. Scanning electron micrograph of a Co(p-Et_2N)TPP film grown electochemically on a Pt electrode at a constant potential of 1.5 V for 10 min; magnification 5000:1.

many craters. A closer look inside the crater reveals a comparatively even compact microspheroid surface morphology, Figure 5b. Contrary to this, the surface of Co-(p-Et_2N)TPP is rougher, with no apparent craters present. The surface also demonstrates microspheroids larger than that seen in the Ru(CO)(p-Et_2N)TPP(t-Bupy) film, resulting in a less compact morphology, Figure 6. A similar surface morphology was also obtained for the Pd(p-Et_2N)TPP film, not shown.

Electrocatalytic Oxidation of Hydrazine. Our studies of the oxidation of hydrazine were investigated by films formed from the free-base and metalated PCPP and T(PCP)P and the metalated (p-Et_2N)TPP on GC electrodes in NaOH. The strategy used in these investigations was essentially straightforward and involved scanning the potential from −0.2 to 1.2 V in 0.1 M NaOH with a GC electrode without film and repeating with the GC/film electrode. This same procedure was then carried out in a solution of hydrazine/0.1 M NaOH in order to ensure that the reaction observed was that of the hydrazine oxidation rather than some redox reaction occurring in the film. The efficacy in electrocatalysis was evaluated by the ΔE in the anodic peak potentials for the oxidation of hydrazine by the film electrode and the oxidation of hydrazine by a GC electrode without film. As the potential of the voltammetric peak potential becomes more negative, in comparison to the oxidation of hydrazine by the GC electrode alone, the greater the decrease in the overpotential of the reaction and the more efficient is the electrocatalysis. For the oxidation of hydrazine on a GC electrode without film, molecular nitrogen was observed as the product of oxidation and the peak potential observed for this reaction, after the subtraction of background, was 0.98 V (Figure 7a).

Previous investigations into the oxidation of hydrazine by various phthalocyanines (Pc) containing VO, Cr, Mn, Ni, Cu, and Zn and their tetrasulfonated analogues (TSP), containing VO, Mn, Cr, Ni, Co, and Zn, attached to ordinary pyrolitic graphite (OPG), have demonstrated catalytic ability in the oxidation of hydrazine and a significant decrease in the overpotential of this reaction by up to 0.7 V, relative to the OPG substrate.[17] These same studies also indicate that the activity of the various incorporated metals decrease in the following order: Mn–Pc > Mn–TSP > Cr–TSP > Ni–TSP > VO–Pc > Ni–Pc, which is approximately the same as Cu–Pc, VO–TSP, and Zn–TSP > Co–TSP > graphite.[17a]

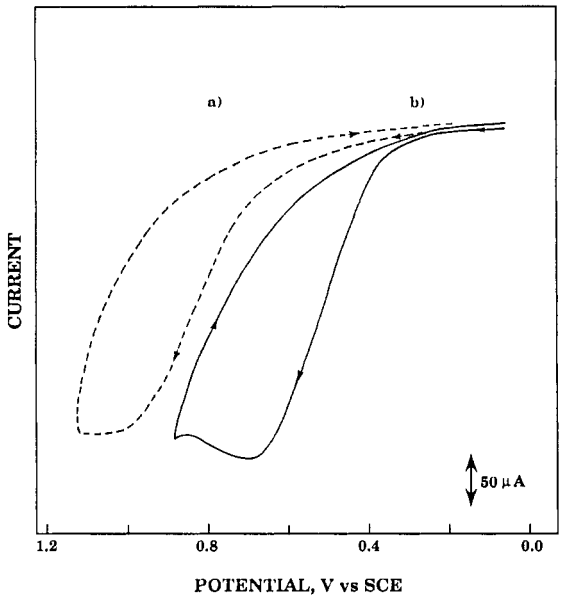

Figure 7. Cyclic voltammograms of the electrooxidation of hydrazine in 0.1 M NaOH: (a) at a GC electrode without film (dashed line); (b) at a poly-T(PCP)P/GC film electrode, $\Gamma = 4.57 \times 10^{-9}$ mol cm^{-2}, $E_{pa} = 0.68$ V.

Table II. Electrooxidation of Hydrazine by Free-Base and Metalated PCPP and T(PCP)P Films on GCE in 0.1 M NaOH

film	$10^9\Gamma$, mol cm^{-2}	E_{pa}, V vs SCE	ΔE, mV
PCPP	3.02	0.40	540
CoPCPP	2.15	0.45	530
	9.20	0.46	520
T(PCP)P	4.57	0.68	300
MnT(PCP)P	1.38	0.65	330
	2.20	0.66	320
	3.45	0.67	310
CoT(PCP)P	1.10	0.56	420
	2.00	0.58	400
NiT(PCP)P	1.12	0.40	540
	2.59	0.35	630

The experimental data for the electrooxidation of hydrazine by the metalated porphyrin films reported here not only indicate a dependence on the metal in regard to the efficacy of the reaction but also clearly demonstrate that the free base of both PCPP and T(PCP)P efficiently catalyze this reaction. Previous research in electrocatalysis has always implied that a metal should be present for successful and effective electrocatalysis, which makes our results difficult to explain. Presumably, the oxidation reaction is influenced and enhanced by a surface type catalytic effect.

Table II presents the results for the oxidation of hydrazine by the free-base and metalated PCPP and T(PCP)P films on GC electrodes in NaOH, which include the film thickness, in mol cm^{-2}, as well as the E_{pa} and the decrease in the overpotential of the oxidation reaction, represented by ΔE. In addition, the voltammogram for this reaction by a T(PCP)P/GC film presented in the table is illustrated in Figure 7b. As can be observed in Table II, the catalytic electrooxidation of hydrazine is governed by the particular porphyrin and central metal involved as well as by the surface coverage, Γ.

In general, a monolayer coverage of the electrode should show similar catalytic effects as a multilayer coverage. However, in the case of polyporphyrins which demonstrate an "island type" of film growth, more than one equivalent monolayer is needed in order to obtain full coverage of the electrode and maximum catalytic effect. Once this maximum point is reached, which depends on the morphology of the specific porphyrin film, further growth results in a decrease in catalytic effect, due to iR loss. Pertinent to this discussion is the fact that these particular porphyrin films are hydrophobic and impermeable in aqueous solution and therefore catalytic or other electrodic reactions occur only on or very near the surface. This was confirmed by measuring the redox reaction of $Fe(CN)_6^{3-}/Fe(CN)_6^{4-}$ in KCl solution with the various porphyrin film electrodes.

Table III. Electrooxidation of Hydrazine by Metalated (p-Et_2N)TPP Films on GCE in 0.1 M NaOH

film	$10^8\Gamma$, mol cm^{-2}	E_{pa}, V vs SCE	ΔE, mV
Co(p-Et_2N)TPP	3.24	0.33	650
	6.47	0.30	680
Ni(p-Et_2N)TPP	0.77	0.34	640
	0.90	0.31	670
	1.74	0.35	630
	3.48	0.46	520
Ru(CO)(p-Et_2N)TPP(t-Bupy)	1.92	0.76	220
	3.20	0.68	300
	4.79	0.57	410
Mn(p-Et_2N)TPP	6.91	0.74	240
	9.06	0.68	300

Table II shows that the activity of the hydrazine reaction by the paracyclophanylporphyrin films decreases as follows: NiT(PCP)P > PCPP > CoPCPP > CoT(PCP)P > MnT(PCP)P > T(PCP)P. While the E_{pa} for this reaction varies in value from 0.68 to 0.35 V, the calculated ΔE range and decrease in overpotential is 300–630 mV. The lowest range in ΔE is demonstrated by the poly-T(PCP)P, MnT(PCP)P, and CoT(PCP)P films, which show peak potentials from 0.68 to 0.58 V, resulting in a ΔE range and decrease of overpotential of from 300 to 400 mV. On the other hand, the ΔE for the poly-PCPP, CoPCPP, and the NiT(PCP)P films range from 520 to 630 mV, with the highest decrease in overpotential achieved by poly-PCPP, ΔE = 540, and the poly-NiT(PCP)P films, ΔE = 540 and 630 mV.

The experimental data for the catalytic electrooxidation of hydrazine by the metalated (p-Et_2N)TPP films on GC electrodes in NaOH are presented in Table III. Similar to the results obtained by the paracyclophanylporphyrin films, the catalytic electrooxidation of hydrazine by the [(diethylamino)phenyl]porphyrin films appear consistent within each porphyrin group and demonstrates a dependence on the porphyrin and the central metal involved, in addition to the surface coverage. For the metalated (p-Et_2N)TPP films, the activity of the hydrazine reaction decreases in the following manner: Co(p-Et_2N)TPP > Ni(p-Et_2N)TPP > Ru(CO)(p-Et_2N)TPP(t-Bupy) > Mn(p-Et_2N)TPP. Also, as shown in Table III, the results cover a broader range and exhibit a greater decrease in the overpotential of the oxidation reaction, related by larger ΔE values, compared to those observed in the paracyclophanylporphyrin films.

In the electrooxidation of hydrazine, the anodic peak potentials range in value from 0.76 to 0.30 V, which result in ΔE varying from 220 to 680 mV. The lowest decrease in the overpotential is found in the Mn(p-Et_2N)TPP films, followed by the Ru(CO)(p-Et_2N)TPP(t-Bupy) films, which show ΔE values from 240 to 300 and 220 to 410 mV, respectively. The highest decrease in the overpotential for this reaction occurs in the Ni(p-Et_2N)TPP and Co(p-Et_2N)TPP films, which exhibit values of ΔE ranging from 520 to 680 mV. The lowest observable E_{pa} for the electrooxidation of hydrazine is 0.30 V for the poly-Co(p-Et_2N)TPP, which is 50 mV lower than the lowest E_{pa}

discerned for the poly-NiT(PCP)P film.

It is interesting to note that the poly-Ni- and -Co-paracyclophanylporphyrin films, as well as the poly-Ni- and -Co-[p-(diethylamino)phenyl]porphyrin films, manifest greater catalytic ability in the oxidation of hydrazine than the Ni-phthalocyanines and the Ni and Co tetrasulfonated phthalocyanines of ref 17. On the other hand, while the MnT(PCP)P and the Mn(p-Et_2N)TPP films demonstrate the least activity in the oxidation of hydrazine, both the Mn(Pc) and the Mn(TSP) exhibit the greatest activity in this oxidation reaction.[17a]

The thin T(PCP)P film, as seen in the scanning electron micrograph, Figure 4, is characterized by a smooth but irregular film morphology with no microspheroidical features and exhibits the least catalytic activity in the oxidation of hydrazine. Although the thicker, caramellike surface of the Ru(CO)(p-Et_2N)TPP(t-Bupy) film, Figure 5a, appears relatively smooth, it contains many craters that are characterized by a compact microspheroid surface morphology, Figure 5b, and catalytically exhibits a medium-range activity in the hydrazine oxidation reaction. Contrasting with these two films is the film of Co(p-Et_2N)TPP, Figure 6, which is rougher with no craters present and exhibits a very high catalytic activity in this oxidation process. Interestingly, the surface morphology of these three films correlates very well with the double-layer capacitance (C_{dl}) data obtained from some impedance spectroscopy measurements.[32] These data demonstrate unusually large C_{dl} values, indicating the presence of quite intricate and rough film surfaces. It would be worthwhile, at this point, to examine the film morphologies of both the free-base and metalated PCPP films, the other metalated T(PCP)P films, and the remaining metalated (p-Et_2N)-TPP films, to see if their surface morphologies parallel the catalytic activity in this particular oxidation reaction.

Conclusions

The results obtained from the catalytic studies presented in Tables II and III clearly demonstrate that the paracyclophanylporphyrin film electrodes and the [p-(diethylamino)phenyl]porphyrin film electrodes play a significant role in the electrocatalytic oxidation of hydrazine.

For the paracyclophanylporphyrin films, PCPP, CoPCPP, CoT(PCP)P, and the NiT(PCP)P all exhibit large ΔE values that range from 400 to 630 mV. Similarly, with the [p-(diethylamino)phenyl]porphyrin films, Co(p-Et_2N)TPP and the Ni(p-Et_2N)TPP manifest the most negative anodic peak potentials, resulting in ΔE values ranging from 520 to 680 mV. Unequivocally, both the Co and Ni paracyclophanylporphyrin films and the Co- and Ni-[p-(diethylamino)phenyl]porphyrin films demonstrate catalytic capabilities in this reaction. The surface morphology of the films discussed also suggest features that may be important in their catalytic activity, especially in the oxidation of hydrazine.

Acknowledgment. We acknowledge and thank Professor Czuchajowski et al., Department of Chemistry, University of Idaho, Moscow, Idaho, for the original synthesis and generous supply of the free-base and metalated paracyclophanylporphyrins.

Registry No. PCPP (homopolymer), 121749-05-1; CoPCPP (homopolymer), 132911-79-6; T(PCP)P (homopolymer), 123785-92-2; MnT(PCP)P (homopolymer), 132938-13-7; CoT(PCP)P (homopolymer), 132938-14-8; NiT(PCP)P (homopolymer), 132938-15-9; Co(p-Et_2N)TPP (homopolymer), 123833-36-3; Ni(p-Et_2N)TPP (homopolymer), 133099-45-3; Ru(CO)(p-Et_2N)-TPP(t-Bupy) (homopolymer), 123833-38-5; Mn(p-Et_2N)TPP (homopolymer), 132938-16-0; hydrazine, 302-01-2.

Composition-Controlled Metal–Nonmetal Transition in $La_{2-x}Sr_xNiO_{4-\delta}$

C.-J. Liu, M. D. Mays, D. O. Cowan,* and M. G. Sânchez*

Department of Chemistry, The Johns Hopkins University, Baltimore, Maryland 21218

Received December 12, 1990. Revised Manuscript Received March 4, 1991

Materials with the general composition $La_{2-x}Sr_xNiO_{4-\delta}$ retain the perovskite-related structure of space group $I4/mmm$ up to $x = 1.50$. They undergo a composition-dependent metal–nonmetal transition in electrical conductivity. The composition parameters x and δ determine the conductivity type. For $x < 1$ the materials are nonmetals. For $x > 1.1$ metallic conductivity is observed that persists to a limit of at least $x = 1.50$ if the oxygen deficiency δ is low. For compositions near the transition the conductivity type is also dependent on δ. Metallic samples become nonmetals upon heating in flowing Ar at 1000 °C, which revert to metals upon oxidation in O_2 also at 1000 °C. All nonmetal-to-metal transitions are accompanied by a change in color from black to reddish brown. The Ni average valence v was determined from the metals composition and iodometric titration data. The δ value was calculated from v by using the equation $\delta = 0.5x + (1 - 0.5v)$, which was derived by using a formal valence convention. Both v and δ increase monotonically with x in the range $0 \leq x \leq 1.5$. A phase diagram is proposed for the metal–nonmetal transition in which the boundary is given by $\delta = 0.5x - 0.51$, which corresponds to $v \approx 3.02$. No stoichiometric 214 nickelate ($\delta = 0$) could be prepared in the metallic region, and no superconductive transition was observed in any material down to ~3 K.

Introduction

Many efforts have been made to increase the transition temperature, T_c, of the ceramic superconductive cuprates and to understand the nature of the new type of conductivity shown by these new materials. One of the tactics used has been to substitute the ionic metals by similar metals. These substitutions preserve the –[CuO_2]– layers within the structure, but they change the interatomic distances as well as the charge carrier concentration and type. Another tactic has been to use other transition metals in the square-planar array. One candidate for this type of approach is $La_{2-x}Sr_xNiO_{4-\delta}$, which is known to form

0897-4756/91/2803-0495$02.50/0